Eurasian Chemico-Technological Journal 16 (2014) 35-39

The Efficiency of the Centrifuge is Force Action on the Propagation Mechanism of SHS-Wave

G.I. Ksandopulo

The Institute of Combustion Problems, 172 Bogenbay batyr Str., Almaty, Kazakhstan

Abstract

Adiabatic wave (AW) is generated by the effect of two forces, namely centrifugal and Coriolis forces, caused on the reaction of the self-propagating high-temperature synthesis (SHS). The synthesis occurs in the aluminothermic oxide system placed inside the heat insulated cylindrical reactor rotating around a vertical axis. Actually there take place two processes during the SH synthesis:

1. separation of the reaction products, in particular aluminum (corundum) oxide concentrated on a quartz wall of the reactor and forming a tube;

2. formation of a coherent flow of liquid metal particles accelerating in the reactor axis direction according to its rotation speed and co-ordinates of R_x particle in the reactor.

The size of the cluster representing particles practically does not change from the very moment of their generation as a result of the reaction due to their motion coherency. Considering the motion speed particles get inside a fresh combustible mixture deeper and deeper and, thus, initiate ignition of the accumulating reaction mixture. This provides growth of the heat release rate and transition of the process to the adiabatic mode.

Metal clusters bearing kinetic energy and heat energy of the reaction (T = 2.8-3.5 thousand K) actually have a high energy potential that can increase according to growth of the rotation speed and longitudinal size of the reactor. So, if any highly endothermic reaction mixture takes place within a reactor co-ordinate with exponential growth of the moving clusters energy this reaction can be initiated and consequently will give start to numerous research capabilities.

A real possibility of such rare and new materials synthesis technology is illustrated using as an example a reaction of the boron and aluminum oxides attacked by 92 m/s speed moving tungsten clusters with formation of a product from the intermediate boron and aluminum oxides and also tungsten and aluminum borides. The results of the synthesized oxide material study using a radio spectrometer has been presented and presence of free valency in it has been identified. Production of free valency materials is of interest in terms of their mixture with nanomaterilas and their compaction at ultrahigh pressure with the purpose to receive new materials with original mechanical, electric, photo-electric, and other properties. The references given below contain data on this technology studied previously.

Introduction

Earlier [1] using the metal particles generating oxide systems as an example,

$$MO_3+2Al \rightarrow M+Al_2O_3+Q \quad (1)$$

We studied factors contributing to the SHS-wave stability in the conditions of the centrifugal force effect. This study allowed for identification of the front propagation features in the cylindrical insulated reactor rotating around a vertical axis [2-6].

There are two forces that affect the liquid metal particles formed in reaction (1) with *m* mass:

1) Centrifugal force F_H directed along R_x radius-vector

$$F_H = 0{,}011\ m \cdot n^2 \cdot R_x$$

2) Coriolis force F_H directed perpendicular to R_x radius-vector

$$F_H = 2\ U \cdot \omega \cdot m$$

* Corresponding author. E-mail: ksand@inbox.ru

where:

R_x – is a co-ordinate and a radius-vector of the SHS wave propagating in the radial direction;

n – is a number of revolutions per minute;

U – is the reactor axis motion speed in the plane direction;

X, У – are axes of the rectangular coordinates system.

One of the features observed during rotation of the reactor (Fig. 1) is separation of liquid and solid phases of the reaction products [2-3] as a result of interaction between specified forces and a hydrodynamic resistance force generated by them.

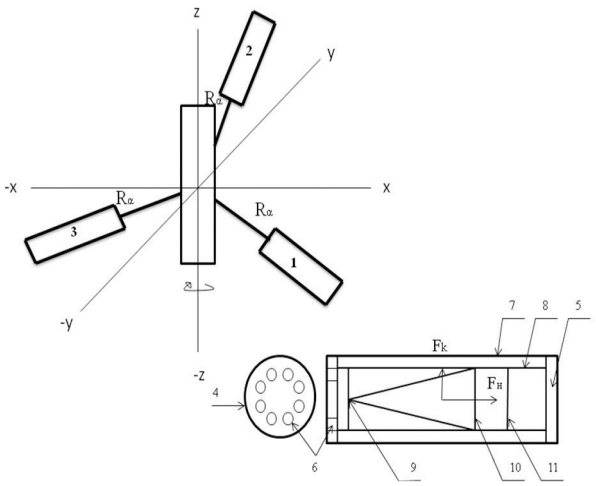

Fig. 1. Diagram of the adiabatic wave producing unit: 1, 2, 3 – rotating reactors; 4, 5 – front and rear reactor covers; 6 – gas outflow holes in the front cover; 7 – steel casing; 8 – quartz; 9 – ignition point; 10 – SHS wave front; 11 – adiabatic wave.

Accelerated movement of the particles along the reactor axis is caused by continuous increment of their R_x rotation radius in the course of the reaction front propagation (Fig. 1). Thus, due to F_H force effect, growth of the particles emerging in the combustion wave front is limited, since their movement becomes coherent. Performed study [4] proves that in the quiescence state the primary size of the metal drops in the reaction similar to (1) is equal to 10^{-6} m. Actually movement of such particles in the quiescence state speed does not depend on the gravitational forces.

Another feature of such SHS-process with fixed rotation frequency is that particles of the reaction metal product emerging at certain critical value R_x develop centrifugal speed Wy that exceeds velocity of U_f ($U_k > U_f$) front thermal propagation. Considering fixed R_x and n values, Tables 1 and 2 illustrate mechanics of the reacting system rotation process during reaction (1) regarding tungsten and iron. For instance, one can see that U_k velocity developed by the tungsten particles along the radius-vector with R_x values = 0.1; 0.25 and 0.3 m, correspondingly, at n = 3000 min^{-1} reaches 30 ÷ 90 ms^{-1}.

The SHS-wave propagation rate in the quiescence state U_f equals only (0.01 ÷ 0.05) ms^{-1}. A typical reaction time in a δ = 0.002 m wide front is τ = δ/UP = (0.1 – 0.04) sec. The contact time of the metal particles running through the front is $\tau = \delta/U = 6.6 \cdot 10^{-5}$ sec ÷ $2.2 \cdot 10^{-5}$ sec. Supposedly, in the rotation conditions hot metal particles (T = 3·103) with over critical[1] speed, continuously get through the front forming ahead a suspended layer i.e. a zone that is spontaneously ignited by the oncoming front heat conductivity. Growth of R_x radius-vector leads to increase in the F_H centrifugal force and size of the self-ignition zone.

1 flow velocity at which a layer resistance becomes equal to its mass.

Table 1
Kinetic energy and enthalpy dependence on the tungsten particle radius and the reactor radius-vector

r·10^{-3}, m	p*10^3, kg/m^3	m*10^{-6}, kg	R_x, m	n, min^{-1}	F, m*kg/s^2	E_k, J	u, m/s	Q, J
0.01	19.2500	0.00008059	0.10	3000	0.00000080	0.08	31.4643	0.0000
0.01	19.2500	0.00008059	0.25	3000	0.00000199	0.50	78.6607	0.0000
0.01	19.2500	0.00008059	0.30	3000	0.00000239	0.72	94.3928	0.0000
0.1	19.2500	0.08059333	0.10	3000	0.00079787	79.79	31.4643	0.0393
0.1	19.2500	0.08059333	0.25	3000	0.00199469	498.67	78.6607	0.0393
0.1	19.2500	0.08059333	0.30	3000	0.00239362	718.09	94.3928	0.0393
1.0	19.2500	80.59333333	0.10	3000	0.79787400	79 787.40	31.4643	39.2891
1.0	19.2500	80.59333333	0.25	3000	1.99468500	498671.25	78.6607	39.2891
1.0	19.2500	80.59333333	0.30	3000	2.39362200	718086.60	94.3928	39.2891

Table 2
Kinetic energy and enthalpy dependence on the iron particle radius and the reactor radius-vector

$r \cdot 10^{-3}$, m	$p*10^{3}$, kg/m^3	$m*10^{-6}$, kg	R_x, m	n, min^{-1}	F, m*kg/s^2	E_k, J	u, m/s	Q, J
0.01	7.8500	0.00003287	0.10	3000	0.00000033	0.03	31.4643	0.0000
0.01	7.8500	0.00003287	0.25	3000	0.00000081	0.20	78.6607	0.0000
0.01	7.8500	0.00003287	0.30	3000	0.00000098	0.29	94.3928	0.0000
0.1	7.8500	0.03286533	0.10	3000	0.00032537	32.54	31.4643	0.0233
0.1	7.8500	0.03286533	0.25	3000	0.00081342	203.35	78.6607	0.0233
0.1	7.8500	0.03286533	0.30	3000	0.00097610	292.83	94.3928	0.0233
1.0	7.8500	32.86533333	0.10	3000	0.32536680	32 536.68	31.4643	23.2516
1.0	7.8500	32.86533333	0.25	3000	0.81341700	203 354.25	78.6607	23.2516
1.0	7.8500	32.86533333	0.30	3000	0.97610040	292 830.12	94.3928	23.2516

The SHS-wave autoacceleration degenerated based on such mechanism actually is a source of the adiabatic wave (AW) and a cause of its thermal instability. It is evident from Tables 1, 2 and Figs. 2-4, and also data [1] that particles kinetic energy exponentially grows with increase in the R_x value.

The purpose of this study is to identify properties of the resulting high energy potential E_C sufficient for initiation of highly endothermic chemical processes since there is a possibility to reach a supersonic AW velocity by variation of n and R_x values.

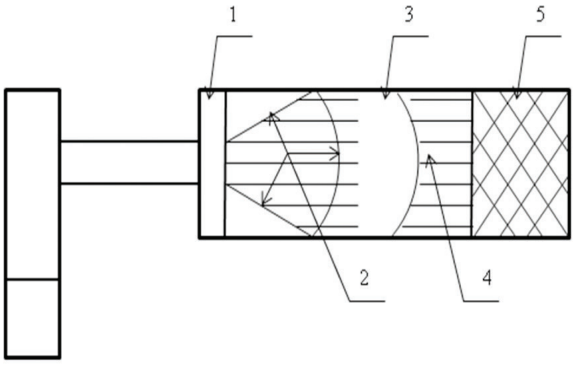

Fig. 2. Technology of AW-based material synthesis: 1 – initiation (ignition); 2 – primary combustion front; 3 – AW generation; 4 – residue of the initial combustible mixture not yet transformed according to (1); 5 – reaction mixture attacked by AW particles.

Energy (AW) and Its Kinetic Ability

At critical R_x point of the SHS-wave transition to AW and further at $R_x > R_k$ when its chemical and kinetic potential is highest, a flow of the attacking particles can be directed arranged so as to initiate highly endothermic reactions. Thus, having combined two different and consistent reaction mixtures within a uniform rotating reactor we have managed to create a new reactor (Fig. 2) able to generate both a sonic and supersonic waves. Calculations have revealed that attacked reaction mixtures in the consecutive phase reactions can consist of two and more various reaction layers.

In a simplified one-phase version of the reactor, the first part is "attacking" similar to reaction (1) for AW generation; whilst the second part is "attacked" with highly endothermic reaction mixture.

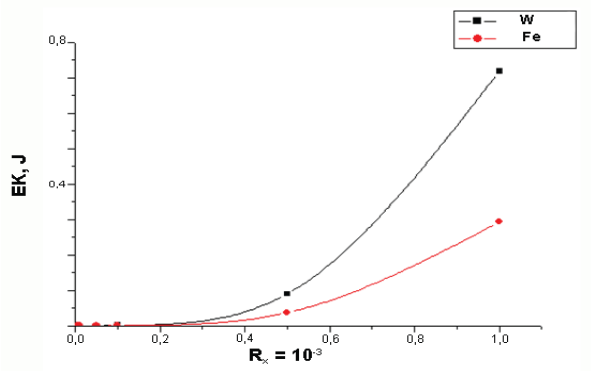

Fig. 3. Tungsten and iron particles kinetic potential within $R_x = 10^{-3}$ m range.

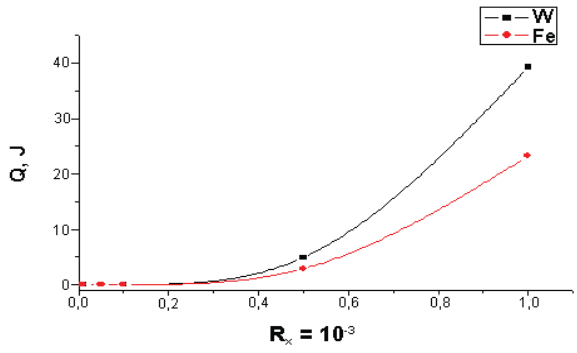

Fig. 4. Heat release in the SHS wave within $R_x = 10^{-3}$ m range.

Using Tables 1-2 and Figures 3-4 one can estimate a total number of N particles with a certain radius $r \cdot 10^{-3}$ m. As an ideal version, we can assume that all particles have the same radius, therefore all tungsten reduced in the first part of the reactor in the amount of 0.045 kg at point $R_x = 0.3$ m will transform to N = 558 particles each with energy $E_k \sim 0.72$ J, its total value being 446 J. Further assuming that an attacked layer thickness is equal to 0.02 m and a particle velocity taken from Table 1.2 is equal to $U = 94.4$ ms^{-1}, the attacking particle contact time in such layer is $\tau \approx 0.02/94.4 \approx 2 \cdot 10^{-4}$ sec. Consequently, capacity of the flow falling onto the attacked layer is $P = 446/2 \cdot 10^{-4} = 2 \cdot 10^6$ W.

Considering that both micro- and macro particles dispersed by the centrifugal force, apart from the translational energy, have a high temperature reaching 2500–3500 K, one can expect to overcome the activation reaction barrier within the attacked layer as a B-O bond rupture approximately equal to 770 KJ/mol [6] even at $R_x = 1 \cdot 10^{-3}$ m. Energy of a chemical bond rupture in the inorganic materials with oxygen does not exceed 1000 KJ/mol in known examples. Therefore performed assessment shows that a total energy of the attacking tungsten particles significantly surpasses this value and, hence, this supposed process is possible. Thus this technology presented as a new project has a considerable chance to increase its capacity with increase of n and R_x values and therefore numerous metals can be used as attacking particles.

Random Examples and Certain Range Sections Covered by AW Technology

Below given are certain idealized trends that are currently being studied [9-10] or can be studied as an attacking reagent, e.g. using tungsten particles as one of the extensive attacking particle examples row with favorably high density. The tungsten particles spectrum within the cluster is rather represented narrow since F_H growth starting from $R_x = R_k$ reduces the coalescence event number. As indicated above, the authors [4] believe that the M^*cluster size at the generation moment is equal to 10^{-5}–10^{-6} m.

Presence of larger particles in the flow is caused only at the start of SHS-process when the highest M^*cluster growth rate is possible due to small F_H value.

$$WO_3 + 2Al \rightarrow Al_2O_3 + W^* \quad (2)$$

$$W + W \rightarrow W_2^* \quad (3)$$

$$W_2 + W \rightarrow W_3^* \ldots . M^* \quad (4)$$

In the absence of details of the macrokinetic mechanism between a liquid cluster and attacked reagent we can judge only based on the actual reaction products. E.g. transformation of a boron oxide and aluminum powder reaction mixture

$$B_2O_3 + 2Al + Q \rightarrow Al_2O_3 + B_2 \quad (5)$$

will start from activation of boron oxide:

$$B_2O_3 + M^* \rightarrow B_2O_3^* \quad (6)$$

and thus will initiate numerous aluminum interaction channels:

$$B_2O_3^* + nAl \rightarrow Al_2O, Al_2O_3, B_2O_3, B_2O, B_2 \quad (7)$$

In turn, emerging aluminum and boron oxides start interacting with each other and resulting in the spinel-like structures and thus reactions of oxygen redistribution between aluminum and boron with formation of various intermediate oxides become possible. Free valencies arising at boron and aluminum atoms can enter layered annular structures. Studies [9-10] demonstrate that formation of WB_2 and AlB as an extreme case is possible as well. An important feature of this complex interaction of three metals in these experiments is absence of attacking metal oxides in the attacked layer, this fact being probably attributed to insufficient particles energy in selected conditions of the experiment.

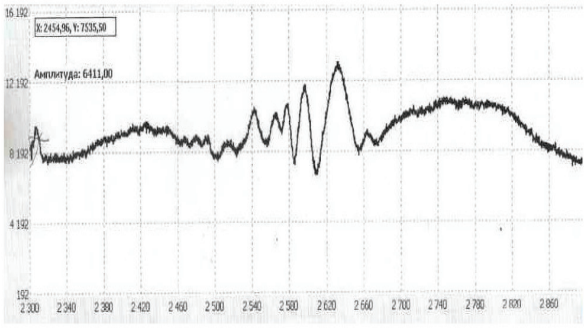

Field center (3) – 3338	Attenuation of SHF (dB) – 20
Field range (3) – 100	Amplification factor – 500
Modulation (m^3) – 5500	Phase – 0
Record time (sec) – 20	Accumulation – 9

Fig. 5.

Figure 5 illustrates data on the EPR sample in reactions (5-8) testifying to occurrence of the free valency in $Al_\alpha O_\beta B_\gamma$ system. The X-ray phase analysis data are also provided in [9-10]. Synthesis of the

bimetallic oxides of sulphides, carbides, nitrides, and other metal oxides (MO) with the perspective to produce free valency materials seems highly promising as there is a chance for numerous combinations with nanomaterials.

$$MgO + Zr^{*} \rightarrow Mg^{*} - O - Zr^{*} \qquad (8)$$

Considering the above mentioned experimental observation that the attacking metal has been absent in the oxidation products, noteworthy that realization of reaction (8) needs more severe conditions to activate the attacking metal, for instance, up to the sound speed or even more.

Apart from that there is a real possibility to use an attacking metal cluster, e.g. with Fe, V (or other elements) so as to initiate a focused polymerization of any monomer with the formation of the electrophysical characteristics gradiency.

Reactions (4) - (9) and a number of similar reactions are extremely useful for production of original materials that are fit for 20-50 thousand atmosphere pressurized «joint» of their mixtures with nanometals as well as other free valency materials. Therefore considered research trend is of potential practical interest in the search for new ways of synthesis of the materials with original mechanical, thermal, photo-electric, and electrophysical properties.

References

1. G.I. Ksandopulo. International Journal of Self-propagating High-temperature Synthesis. 4 (20) (2011) 220-223.
2. A.M. Ainabaev, M.P. Arkhipov, A.N. Baydeldinova, K.I. Omarova, G.I. Ksandopulo Out of Furnace Synthesis of High-Temperature Ceramic Materials in the Revolving Reactor. 2nd International Conference on Competitive Materials and Technology Processes. – Micds – Lillafured, Hungary. – 2012. – P. 139.
3. G.I. Ksandopulo, A.N. Baideldinova, V.N. Shevchenko, G.G. Ksandopulo. High-Temperature Centrifuge. RoK Patent No 68316 as of 26.05.2010. Innovative RoK Patent No 23988 as of 26.05.2010.
4. A.I. Kirdyashkin, V.D. Kitayev, V.G. Salamatov, R.A. Yussupov. Physics of Combustion and Explosion. 44 (1) (2008) 80-84.
5. G.I. Ksandopulo, A.N. Baideldinova, A.M. Ainabaev, M.P. Arkhipov, K.I. Omarova. Eurasian Chemical-Technological Journal. 13 (3-4) (2011) 155-160.
6. Reference Book. Energy of Chemical Bond Rupture. Ionization Energies and Electron Affinity. - M: USSR Science Academy Publ., 1962.
7. G.I. Ksandopulo, G.G. Ksandopulo. High-Temperature Centrifuge for Metallothermic Smelting of Ferroalloys. RoK Patent No 23989 as of 16.05.2011.
8. G.I. Ksandopulo, A.N. Baideldinova, G.G. Ksandopulo, A.M. Ainabaev, M.P. Arkhipov Method of Metals and Ferroalloys Production. RoK Patent No 68565 as of 26.05.2010.
9. G.I. Ksandopulo. Gorenie i plazmohimija [Combustion and plasmochemistry]. 2013. p. 20-22.
10. A.N. Baideldinova, K.I. Omarova, B.Zh. Nurakhmetov, N. Sabyrov, G.I. Ksandopulo. Combustion and plasmochemistry. – Almaty. 2013. p. 164-167.

Received 30 September 2013